ARTICLE

Micro-Flow Synthesis Of A Formulation Of Phosphorus Fertiliser To Enhance P Content In Soil And P Uptake In Wheat

Received 00th January 20xx,
Accepted 00th January 20xx

DOI: 10.1039/x0xx00000x

Tu Nguyen Quang Le,[ab] Karen Robertson,[c] Marc Escribà-Gelonch,[de] Petra Marschner,[f] Nam Nghiep Tran,[ag] Philip Michael Williams,[h] Ian Fisk,[bi] Volker Hessel,[*aj]

Highly soluble commercial phosphorus (P) fertilisers have been the most common form of P applied in agricultural for decades, but their releasing efficiency can be low because phosphate ions can be easily bound with cations in soil to form precipitates or highly water soluble species, leaching into nearby water sources causing eutrophication. Using the coiled flow inverter (CFI), a new formulation of phosphorus fertiliser was prepared containing three main components: a solid P source (biphasic calcium phosphate), a soil remediation agent (citrate ions) and a binding agent (chitosan). Our paper is one of the first fertiliser performance material made in flow that is a finished product comprising structural and functional complexity and we demonstrate its performance by soil experiments. We show proof of concept at scale to a complex product, which is amenable to open door to a commercial application. The key factors to evaluate the prepared fertiliser were P releasing efficiency, soil available P and P uptake. The prepared formulation tripled the available P in soil applied with commercial apatite (probability value, p-value < 0.05) and reached the same level with commercial P fertiliser in the incubation experiment. After incubating for 14 days, 63% of the applied P in the prepared fertiliser was released in the soil. The formulation without chitosan exhibited higher uptake of P in Scepter wheat in comparison with phosphate rock. In the soil column experiment, the commercial P fertiliser leaked double the amount of phosphorus after 23 days and had a fluctuated releasing behaviour when compared with the prepared formulation. Bacth and flow synthesis (8 mL min^{-1}) share similar green chemistry metrics, including E-factor of 0.4 kg kg^{-1}. Continous-flow production for CS-ACP-Cit has higher productivity than batch by a factor of 1.9. Circularity of the process, denoted by Materials Circularity Indicator (MCI), when considering experimental recycling data, is high for all process steps and all composites, scoring in the range of 0.8; also seeing this is a non-optimised process. The circularity assessment took account for performance of composites, which is expressed as Intensity Factor (U; performance) and Lifetime (L) of the Materials Circularity Indicator (MCI).

I. Introduction

In agriculture, phosphorus (P) is a major growth-limiting nutrient which contributes towards the development of crop including but not limited to root development, stalk and stem strength, flower and seed formation, crop maturity and production, crop quality and resistance to plant diseases.[1]

The original processes for preparing water soluble P fertilisers (SSP, TSP, DAP) from mined phosphate rock are still widely used in the present time.[2, 3] However, P releasing from commercial products also faces fixation in soil solution caused by cations in soil such as Ca^{2+}, Al^{3+}, Fe^{3+} which converts P into a less available form and greatly hinders the P releasing efficiency (PRE); often only 10-15% of the total amount of P is ultimately applied to the soil in a form that can be absorbed by crops.[4] Furthermore, good solubility in these fertilisers also has negative effect on the environment as P in these fertilisers has high mobility which ends up in nearby water bodies through runoff or seepage which causes eutrophication.[5, 6] Unlike other fundamental elements for life such as carbon, nitrogen, oxygen or hydrogen, phosphorus cannot circulate in the biosphere due to having no significant gaseous phase. Thus, phosphorus is a finite source that can take millions of years to render and accumulate in the earth's crust before it can be explored and used for human activities. We can tackle this problem *via* two approaches: to find more or to use less. In term of finding more, we can look beyond the stars and find new place rich in P, such as lunar soil that is rich in KREEP (K – potassium, REE – rare earth element, and P – phosphorus) or to use recycling technology to recover P from biowaste such as roots.[7, 8] The idea of using less means use a P fertiliser that releases nutrient slowly or under a controlled manner. Solid P fertiliser, such as hydroxyapatite (HAp), where

---

[a] *School of Chemical Engineering and Advanced Materials, The University of Adelaide, Adelaide, SA 5005, Australia.*
[b] *Division of Food, Nutrition and Dietetics, School of Biosciences, University of Nottingham, Loughborough, LE12 5RD, UK.*
[c] *Faculty of Engineering, University of Nottingham, Nottingham, UK.*
[d] *Department of Chemical Engineering and Chemistry, Eindhoven University of Technology, De Rondom 70, 5612 AP Eindhoven, The Netherlands*
[e] *Laboratoire de Génie des Procédées Catalytiques, Centre National de la Recherche Scientifique (CNRS)–UMR 5285, CPE Lyon, 43 Bd du 11 Novembre 1918, Villeurbanne, France*
[f] *School of Agriculture, Food and Wine, The University of Adelaide, South Australia 5005, Australia.*
[g] *School of Chemical Engineering, Can Tho University, Can Tho City, Vietnam.*
[h] *School of Pharmacy, University of Nottingham, Nottingham, UK*
[i] *The University of Adelaide, North Terrace, Adelaide, South Australia, Australia.*
[j] *School of Engineering, University of Warwick, Library Rd, Coventry, UK*

P is locked in a solid form and thus less soluble has also captured great attention recently as it is advantageous in countering run-off or eutrophication.[9-14] One of the major remaining problems of using hydroxyapatite as a fertiliser is its ability to match the crop needs because of its low solubility of $10^{-52.8}$ at pH = 7.6.[15]

In the light of the problems related to conventional P application, nanotechnology for application in agriculture could hold the answer to effectively provide the nutrient P as the high-quality fertilisers but minimise the environmental risks and match the nutrient need of crops.[16-18] Preparing nano size hydroxyapatite particles can be an effective strategy to increase the solubility and the mobility in soil.[19] Liu and Lal reported the increase in growth rate (by 32.6%), seed yield (by 20.4%) and biomass (by 18.2%) of soybean applied with apatite nanoparticles compared to regular P treatment.[19] Tang and Fei tested the PRE of hydroxyapatite based nanostructured phosphorus fertiliser on the growth of water spinach and observed that the PRE of HAp NPs doubled that of chemical fertiliser.[20] Elsayed et al. also stated that HAp NPs enhanced growth parameters, essential oil yield, stem diameter, fiber thickness of rosemary compared to NPK.[21]

In addition to the formation of fertiliser nanoparticles, a group of substances that received great attention in disrupting the P fixation is low molecular weight organic acids (LMWOAs) or their anions, as they can replace PO_4^{3-} in binding with polyvalent cations in the soil solution. Plants can release organic acid anions from roots which can reduce the number of potential binding sites with P in mineral soils *via* complexation between sesquioxides and organic ligands.[22-25] Theses anions can further enhance P availability by replacing P from biding sites (anion exchange) and the process can be simply demonstrated.[26, 27] However, studies have shown that plants would likely exhibit trade-offs (e.g. resources allocation, carbon costs, photosynthetically fixed carbon) to evolve the strategies to cope with low soil P availability.[28] Thus, by applying an appropriate amount of LMWOAs along P fertiliser, we can optimise the impact on the soil P availability and reduce Al-toxicity in acid soil for future crops.[29, 30] However, when applying to the soil, LMWOAs are rapidly decomposed by microbes, specifically, 50% of LMWOAs can be decomposed after applying for a few hours.[24, 30] The preparation of droplets, or later biodegradable polymeric capsules, can prolong the existence of LMWOAs in the soil.

Chitosan possesses the ability to form gels and films of chitosan due to its cationic nature, by having amino ($-NH_2$) and hydroxy (-OH) functional groups in its structure, and thus opens potentials in using as coating material with high water holding capacity for a wide field.[31-35] Several studies have investigated the addition of a wide range of nutrient in chitosan nanomaterials for their slow/controlled release and their impacts on the plant performance.[36-38] The preparation of modified chitosan membranes using low molecular ionic crosslinking agents such as trisodium citrate, sulfuric acid and pentasodium tripolyphosphate have been reported.[39-42] The combination of citrate ions and chitosan holds great potentials as fertiliser for acidic soil or soils that contain large amount of precipitated P as citrate ions are ranked highest among the LMWOAs in terms of performing the function of releasing fixated phosphate ions in soil.[25]

Compared to conventional batch reactors, microfluidic reactors perform chemical processes under a continuous-flow manner with constant product quality over time, rapid heat and mass transfer at a very low consumption of reagents and more.[43] Additionally, the enclosed environment of microfluidic reactors allows the performance of extreme condition reactions.[44-46] This technology has been demonstrated in many processes, over more than two decades,[47] namely extraction,[48-51] photocatalytic reaction,[52-54] nanoparticles synthesis.[55-59] The coiled flow inverter reactor can enhance the axial mixing and narrow the time distribution due to the convection flow, leading to the narrower particle size distribution.[60] When working with precipitation or crystallisation processes in microfluidic systems, the residence time and fast mixing play an important role in defining the morphology of the material.[61] In a study on the co-precipitation synthesis of stable iron oxide with NaOH, LaGrow *et al*. found that the iron oxide nanoparticles (IONPs) collected at the outlet of a T-mixer exhibited intermediate phases and required an additional aging step in a vessel to transition to magnetite.[62] The study of Besenhard *et al*. showed that the agglomeration of IONPs occurred simultaneously with the co-precipitation reaction after the T-mixers and these agglomerates were too large to achieve colloidal stability.[63] The addition of a coiled flow inverter achieved a stable colloidal flow which increased the intensity of resultant magnetite peaks by ~35% and allowed the addition of citric acid solution without any intermediate steps to facilitate the de-agglomeration.[63] In terms of economic efficiency, continuous crystallisation/precipitation can offer a number of considerable advantages including efficiency usage of energy and materials, smaller footprint, reducing capital and operational expenditure.[64-66] A case study done by Lawton *et al.* showed that by eliminating the variability from batch to batch and producing uniform particles, the post-synthesis processing, namely milling, could be avoided i.e., higher process simplicity, and this resulted in a reduction in the capital costs by 50% and further reduced costs in personnel, milling losses and other inefficiencies by over £300k per annum. [67]

The combination of citrate/apatite or citrate/chitosan has been reported in previous literature but they were largely reported separately and in the context of batch production.[68-72] More often than not, the citrate ions only played a supporting role in these studies as a spatial orientation agent for the growth of apatite crystal[73-77] or a cross-linking agent for the formation of chitosan film/coating.[78-81] There are hardly any reports on making fertilisers by flow chemistry. Gloria et al. reported the use of biomimetic calcium phosphate as a slow-release fertiliser and the citrate ions were only used to mimic the composition of bone nanoparticles.[82] In this regard, this study involved the use of multireactor network and combining, for the first time, flow chemistry steps and chemistries to form a controlled-release fertiliser from the crosslinking of chitosan (CS) encapsulating a limited soluble P fertiliser and citrate ions. The continuous flow system implemented in this study allowed the rapid preparation of the P-containing composites and controlling the size over the batch method. Solid phosphorus, citrate ion and chitosan will each have a distinctive role in improving the performance of the solid fertiliser. The three chosen parameters as P releasing efficiency (PRE), P availability (PA) and P uptake (PU) of crop were evaluated in corresponding with a commercial soluble P fertiliser (Richgro Super Phosphate). It also determined the controlled release behaviour and the leaking risk of the prepare composite in the soil column experiment.

While our experiments use existing chemistries in single steps, these are combined into a multireactor network for the first time. In this way, a new material is created for a new function (performance), which is composite comprising structural and functional complexity. While microfluidic chip devices have been reported to produce complex materials, their practical application lacks due to missing synthesis capability.[83] Some papers have reported on precipitation by flow chemistry, but most produced nanoparticles that are in terms of production scale and performance far from a commercial application.[46, 84-86] We show proof of concept at scale to a complex product, which is amenable to open door to a commercial application. For the application considered, fertilisers, hardly any reports were made using flow chemistry; a very few papers use continuous-flow devices of mixed origin to target fertigation, while not primarily making fertilisers.[87-93] Our paper is one of the first to produce a performance chemical, a flow-made fertiliser composite that is a finished product, as we demonstrate by soil experiments. The relevance of 'performance' and 'effectiveness' in a holistic way for Green Chemistry has been emphasized by the founding father of Green Chemistry Paul Anastas; we need to "understand that we have to look at the entire system".[94]

II. Experimental

2.1. Experimental

Calcium chloride anhydrous ($CaCl_2$, >99% pure, Sigma Aldrich), sodium dihydrogen orthophosphate dihydrate ($NaH_2PO_4.2H_2O$, >99% pure, Chem-Supply), trisodium citrate dihydrate ($(Na_3C_6H_5O_7).2H_2O$, >=99% pure, Chem-Supply), sodium hydroxide (NaOH, >=98% pure, Sigma Aldrich), hydroxyapatite (>= 97% pure, Sigma Aldrich) and chitosan (~3300 kDa, Degree of Deacetylation: ≥ 90.0%, Xi' An Lukee Bio-Tech Co. Ltd) were purchased and used for this study. All solution were prepared with ultrapure water (Milli-Q, Millipore).

2.2. Preparation of composites

Calcium phosphate nanoparticles (ACP). Calcium phosphate nanoparticles were obtained by performing a precipitation reaction (Table S1.) between calcium chloride (0.5 M) and sodium dihydrogen phosphate (0.3 M) in a basic solution (NaOH). The reaction was performed in a simple flow system consisted of Y and T junctions connected with a coiled flow inverter (CFI), as shown in Fig. 1 The CFI was made by coiling a PFA (perfluoroalkoxy) capillary tube (1 mm ID and 2.5 m length) around a 2.5 cm OD cylindrical steel bar that was welded to a square shape (10x10cm). Reagents were introduced to the system using syringe pumps, the 90° bends of the square shape enabled the direction of the centrifugal forces to change 3 times causing even more efficient mixing. The flowrate ratio was 1:1:1 with the total flowrate of 3 mL/min and the reaction was carried out at room temperature. Solid ACP was collected after centrifugation of the solution (3000 rpm, 6 min) and was dried in an oven at 40 °C overnight.

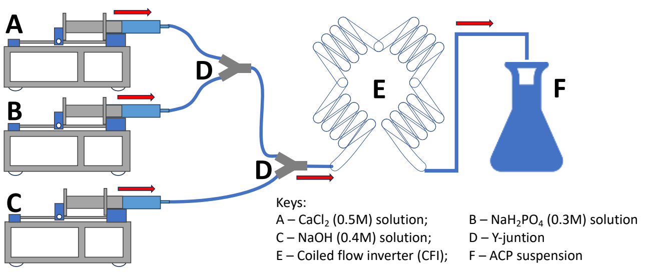

Fig. 1 Schematic illustration of the CFI system for ACP sample preparation

Phosphate – citrate composite (ACP-Cit). To obtain the phosphate-citrate composite, we adapted the previous procedure with a flow of sodium citrate (0.25 M) connected to the system *via* a T-junction connector (Fig. S1). The flowrate ratio was 1:1:1:1 with the total flow rate of 4 mL/min. The final product was collected as described before and was denoted as ACP-Cit

Chitosan – phosphate – citrate composite (CS-ACP-Cit). To further increase the citrate content, the chitosan solution (0.3 %wt in 1% (v/v) acetic acid) was introduced into the system (Fig. S2). The flowrate ratio was Ca^{2+} : PO_4^{3-} : OH^- : $Citrate^{3-}$: Chitosan = 1:1:1:1:4 and the two values of total flowrate investigated (8 mL min^{-1} and 12 mL min^{-1}). The final products were obtained as described before and were denoted as CS-ACP-Cit-8 or CS-ACP-Cit-12.

Batch synthesis. To compare composition in the composite, in parallel with the flow system, a batch reaction was also performed. Calcium chloride (10 mL, 0.5 M) and sodium dihydrogen phosphate (10 mL, 0.3 M) was mixed at the molar ratio of Ca^{2+} : PO_4^{3-} = 5 : 3 in a beaker using the magnetic stirrer. Sodium hydroxide (10 mL, 0.4 M) and trisodium citrated (10 mL, 0.25 M) were added dropwise into the mixture and mixed for 10 minutes. Later, a solution of chitosan (40 mL, 0.3 %wt) was added dropwise into the white suspension and the reaction was allowed to stand for another 10 minutes. The solid collected from the centrifugation of the mixture (3000 rpm, 6 min) was dried in the oven at 40°C overnight.

2.3. Characterisation methods

Laboratory X-ray powder diffraction (XRD) data were collected on a Rigaku MiniFlex 600 X-Ray Diffractometer using Cu Kα raditation (λ = 1.5418 Å), from 20° to 80° (2θ) with a scan rate of 6 s $step^{-1}$, step size of 0.02° with an HV generator set at 40 kV and 15 mA. Particle size distribution was determined by using the Mastersizer 2000 (Malvern, UK) laser diffractometer. An ultra-high performance liquid chromatography (UHPLC) with a diode array detector (Agilent, US) was used to analyse content of chitosan, citrate in the prepared composites. Scanning electronic microscopy (SEM) images were collected with a SEM Hitachi SU7000 Ultra-High-Resolution FE-SEM (Adelaide Microscopy, The University of Adelaide) operating at 20 kV. The composite collected by centrifugation were ultrasonically dispersed in ethanol, and then a few drops of the slurry were deposited on a thin amorphous carbon film.

Table 1. *Characterisation of the soil sample*

Soil texture	pH($CaCl_2$)	Water holding capacity (g/g_{soil})	Total organic carbon (TOC) (%)	Available P (mg/kg_{soil})	Total P (mg/kg_{soil})
Sandy loam	5.6	0.23	1.69	16	266

2.4. Soil collection and characterisation

The soil used in this study was collected from a wheat paddock of Condowie SA (-33.75648676, 138.39642). The soil was dried in the oven at 40°C and was sieved through a 10-mesh sieve prior to use in the soil column and soil incubation experiments. The soil characteristics were analysed using the corresponding methodology at Waite Campus, University of Adelaide, Australia and are summarised in Table 1.

2.5. P uptake experiment: the case of phosphate-citrate composite

The P uptake was investigated *via* wheat growth experiments conducted in a greenhouse at Waite Campus, the University of Adelaide. The soil used in these experiments was oven dried over at 40 °C and was sieved through a 10-mesh sieve (2 mm) to control the uniformity. The soil mixtures were prepared with 50% of the maximum water holding capacity and a starter fertiliser consisting of urea (50 kg N ha^{-1}); KCl (50 kg K ha^{-1}), a second dose of urea (50 kg N ha^{-1}) was applied at the third week. The application doses of P, in the form of phosphate-citrate composite, were varied from 0 to 30 kg P ha^{-1} with the starter fertiliser. The pots were weighed and watered every 3 days to maintain a consistent water fraction during the duration of experiment. Scepter wheat was kindly provided by the university laboratory (denoted as Type I) and local farmer (denoted as Type II) for the experiment. The seeds were pre-germinated without light for 48 hours before sowing. The most uniform seeds were sown to the pre-mixed pot at the rate of 5 seeds per pot at 30 mm depth according to a master plate position. Then, the seedlings were thinned to 3 per pot at 2-leaf growth stage by leaving the most uniform seedlings in each pot. The time of harvest was 8 weeks, during this, the height of the wheat was recorded every 3 days. At harvest, the shoots were separated from the roots at the soil surface and the roots were recovered from the soil. The shoots and roots were washed to remove the soil and were oven dried until the weight remained constant. The dried biomass was then prepared for analysis of P content *via* acid digestion and analysed using a UV-Vis spectrometer. The P uptake in biomass was calculated as follow:

$$P_{uptake} = \frac{Total\ P\ in\ biomass}{Total\ mass\ of\ soil\ per\ pot}$$

2.6. Soil incubation experiment

The soil incubation experiments were conducted to investigate the ability to enhance the P availability and the P releasing efficiency of the material. Generally, appropriate amounts of fine powders (apatite(sigma-aldrich), commercial fertiliser, sodium citrate, ACP-Cit, CS-ACP-Cit) were added to a small pot containing 50 g of soil so that the P application rate was 25 kg P ha^{-1}. The soil was first watered to reach half of its maximum water holding capacity and was water again every 48 hours to maintain the same weight. The experiment was conducted in the green house for 14 days. At the end of the experiment, the soil was dried in an oven at 40°C overnight and was analysed for P content by UV-vis spectrophotometry using the Colwell method.[95]

The available P in soil is defined as the amount of P that will be available for plant uptake and can be directly compared with the control condition (no fertiliser) from Colwell method. The P releasing efficiency (PRE) is defined as the percentage of P nutrient from the fertiliser that is still available to the plant in the incubation experiment. This efficiency for commercial nutrient is commonly less than 100% due to leaching or precipitation or fixation with other elements in the soil media. The PRE was calculated as follow:

$$PRE = \frac{Phosphorus\ output}{Phosphorus\ input}\ (\%)$$

Where, Phosphorus output = total P available in the soil
Phosphorus input = total P in fertiliser + soil supply of P

2.7. Soil column experiment

Experiments were performed in vertical column filled with sieved soil and a corresponding amount of composite/fertiliser (phosphate, commercial fertiliser and chitosan – phosphate – citrate composite) at the P application rate of 65 $mg_P\ kg_{soil}^{-1}$. The columns were made of PE cylinder tubes (120 mm length and 30 mm ID) with the bottom covered with filter paper to prevent fine particles from leaching out. The soil was packed at a 10 cm depth and was then weighed to determine the corresponding dose for each type of fertiliser. The column was watered with ultrapure water until reaching water holding capacity. Then, ultrapure water was poured into the column at volume of 5 mL every 24 hours. At 17:00 every day, the leachate from the column was collected and filtered through a 0.25 µm membrane filter. The P content of the leachate was calculated based on the leachate volume and the P concentration obtained by UV-vis spectrophotometry using the Colwell method as follow:[95]

$$P\ content = P\ conc. \times V_{leachate}$$

Where, P conc. = P concentration in leachate (µg/mL)
$V_{leachate}$ = *Volume of leachate (mL)*

2.8. Data analysis and statistics

One-way analysis of variance (ANOVA) was performed to calculate the effects of fertiliser type on the available P and P releasing efficiency (PRE). Two-way ANOVA was performed to investigate the impact of treatment in the wheat growing experiments and the soil column experiments. The p-value < 0.05 was considered as the threshold value for statistical significance. Tukey's studentised range test was chosen as the post-hoc analysis of treatments.

III. Results and Discussion

3.1. Composites prepared *via* flow system

The key components of the proposed composites include a solid P composite as a slow-release source, low molecular weight organic acid anions as additives for ion-exchanging and a bio-compatible coating. The composition of the prepared composites is summarised in Table 2. The amounts of composites and commercial fertiliser were calculated based on the phosphate weight percentage from Table 2 to have the same application doses for each type of experiment. At first glance, the prepared composites presented all the key components in the proposed formula (chitosan, phosphorus, and citrate ions) as shown in the CS-ACP-Cit samples. The citrate/phosphate mass ratio was then obtained from the data in Table 2 and are presented in Fig. 2. Compared to the composite without chitosan, the addition of chitosan had impacted the mass ratio of citrate ions and phosphate ions (PO_4^{3-}) as this ratio changed from 0.36 to 1.07. This ratio was increased by increasing the total flowrate from 8 mL min^{-1} to 12 mL min^{-1} in the CFI, yet this only increased to 1.36 while exchanging for a higher chitosan wt% in the final product, from 19.3 ± 0.7% to 30.1 ± 0.7%. Increasing chitosan content may pose an adverse effect as it would take longer for the chitosan to be decomposed and thus longer for the nutrient to be released into the soil. A corresponding procedure for preparing the CS-ACP-Cit-8 under batch conditions was implemented and resulted in a lower citrate/phosphate mass ratio, at 0.73.

The XRD pattern of the ACP sample prepared *via* the coiled flow inverter (CFI) indicated the mixture of the hydroxyapatite (HAp) (JCPDS no. 09-0432) and β-$Ca_3(PO_4)_2$ (β-TCP) (JCPDS no. 09-0169) with the HAp/β-TCP ratio of 14.4 calculated from the reference intensity ratio (RIR) (Fig. S3). The presence of citrate ions impacts the crystal structure of apatite in ACP-Cit and CS-ACP-Cit as the diffraction peaks become broad and poorly defined. Previous studies have shown that citrate ions may incorporate into ACP or adsorb on the surface of ACP, thus changing the crystal structure of the ACP (Table S1). [96] In the context of this study, citrate ions were introduced simultaneously with the precipitation of ACP in microflow to maximise the ratio of citrate/phosphate in the final composite (Fig. 2) due to the higher mixing efficiency in the microchannel in comparison with batch. Chitosan and citrate ion will also react instantaneously *via* cross-linking reaction (Table S1) and microchannel allows this reaction to happen at a control ratio between both reagents, while there is a higher possibility in batch mode that either the chitosan will grow larger or less ACP-citrate coated as the reaction will occur at the interface of the solution and the chitosan droplet.

The ACP prepared from the CFI had one peak in the size distribution (0.8 to 22 µm) which was similar to a commercial apatite purchased from Sigma Aldrich (Fig. S4). The composites prepared *via* the CFI were smaller that of batch method by a factor of 10. The reduction in size for the reported formulation, prepared *via* CFI, decreased the effect of localisation of fertiliser when applied to the soil, as the distribution of fertiliser per area of soil will be greatly enhanced at smaller size. The limited dimensions and the rapid reaction time in the microtube supports a rapid cross-linking reaction of chitosan and reduce the possibility of continuous growing on the chitosan coating, while this requires large energy consumption in the form of agitation speed to achieve the same effect in batch reaction.[97, 98] For samples containing chitosan, it should be noted that the sizes will reflect their swollen size as chitosan absorbs water into the structure and thus their dried particles should have a smaller diameter.

The XRD pattern in section 3.1. also predicts the amorphous of the two latter samples: ACP-Cit and CS-ACPC-Cit which are confirmed in the SEM images (Fig. S3). The ACP sample had the most well-defined morphology among three types of composites. This change of particle shape was also observed in a previous study using citric acid to modified hydroxyapatite by Samavini et al.[99] The particle size of ACP-Cit and CS-ACP-Cit obtained from SEM images were 250-1000 nm and 2.5-30 µm, respectively. The difference in the DLS results and SEM images came from the fact that the chitosan in the composite swell in aqueous medium due to its ability to absorb water, thus making the size distribution in DLS larger than that collected from SEM images.

Table 2. *Composition of the prepared composites*

Sample	P element wt%	Citrate wt%	Chitosan wt%
ACP	18.2 ± 0.2	n/a	n/a
ACP-Cit	15.4 ± 0.1	16.9 ± 0.3	n/a
CS-ACP-Cit-8	6.9 ± 0.2	22.4 ± 0.4	19.3 ± 0.7
CS-ACP-Cit-12	5.3 ± 0.1	22.3 ± 0.2	30.1 ± 0.7
Commercial P	9.1	n/a	n/a
Batch-CS-ACP-Cit	8.8 ± 0.1	19.7 ± 0.1	19.6 ± 0.9

n/a: undetectable

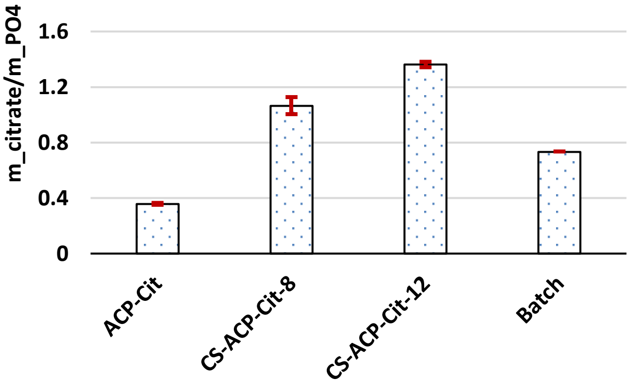

Fig. 2 Citrate ion/phosphate mass ratio of the prepared composites: Phosphate-citrate (ACP-Cit); Chitosan-phosphate-citrate (CS-ACP-Cit-8 and CS-ACP-Cit-12)

3.1.1. Green chemistry metrics for composites manufacturing

New chemical and manufacturing processes need early-stage evaluation by metrics to guide their further optimisation to meet green chemistry and circularity postulates.

To understand these metrics, as presented below, the process settings and innovation of this study needs to be considered. Demonstrated innovation is to produce smaller P nanoparticles in flow than in batch, as commonly reported by flow chemistry studies. This increases the solubility of nano-P and also the homogeneous distribution of dissolved P in soil as transport medium. Both effects boost the performance (effectiveness) of nano-P composites. Compromises in terms of using slightly more material and more water solvent have been made in order to achieve the improved performance of nano-P composites produced *via* the current flow settings. Moving from ACP to CS-ACP-Cit requires the addition of a flow stream for each reagent, while reactants in batch can be added from solid state. Moving to CS-ACP-Cit-12, the total flow rate had to be set higher than for CS-ACP-Cit-8 by a factor of 1.5. Viscosity limitations (aka pressure drop) of performing flow operation demanded to lower chitosan concentration below 1 %wt, which also increased the flow rate. Therefore, pros for the product and cons for the process imply to use metrics which reflect that; green chemistry metrics are on process, circularity metrics are on product.

Green chemistry metrics were calculated in a gate-to-gate fashion, normalising all scenarios for the production time equivalent to completion of a batch process (20 min). The computed green chemistry metrics for the diverse composites of this study are summarized in Table 3; global green chemistry metrics in Table 3a, while specific green chemistry metrics for each ingredient forming the fertiliser product are in Table 3b. The ingredient-specific yield is calculated as the ratio of the mass of fertilizer ingredient per mass of ingredient in the feed; for Ca, P, Cit, and CS.

Green chemistry metrics E-factor measures the waste generated in the process including by-products. Mass intensity (MI) scores on the total mass input of materials (excluding water) normalised by mass output of product. Process mass intensity (PMI) measures the same quantity as MI but considering water (if used). Process mass efficiency (PME) relates the mass of the product to the mass of all feed ingredients, including water. Water intensity (WI) scores the mass amount of water used per mass of product.

Continuous-flow processing results in almost equal global green chemistry metrics as batch processing when comparing CS-ACP-Cit-8 with CS-ACP-Cit, respectively. The productivity of continuous-flow is almost double to batch. The metrics for CS-ACP-Cit-12 are worse as compared to CS-ACP-Cit-8 and batch-made CS-ACP-Cit; yet the productivity of CS-ACP-Cit-8 is almost double to batch.

Table 3. *Sustainability metrics of the composites preparation; green chemistry metrics for global process view (a), and ingredient-individual metrics for specific functional view, as defined in the text (b).*

a) Global green chemistry metrics

	E-factor kg kg^{-1}	PMI kg kg^{-1}	MI kg kg^{-1}	PME %	WI kg kg^{-1}	Productivity g h^{-1}
ACP	1.11	28	2.70	3.59	68	6.46
ACP-Cit	0.93	34	3.89	2.97	81	7.13
CS-ACP-Cit-8	0.40	108	3.72	0.93	146	4.46
CS-ACP-Cit-12	0.40	161	5.59	0.62	310	4.47
Batch-CS-ACP-Cit	0.40	100	3.59	1.00	145	2.46

b) Specific green chemistry metrics (Ca=calcium, P=phosphorus, Cit=citrate, CS=chitosan)

	Ca	P	Cit	CS	Ca	P	Cit	CS
	Yield, %				PMI , kg kg^{-1}			
ACP	83	97	-	-	65	66	-	-
ACP-Cit	78	95	21	-	92	90	263	-
CS-ACP-Cit-8	37	39	25	84	390	442	439	796
CS-ACP-Cit-12	17	23	19	99	827	757	580	659
Batch-CS-ACP-Cit	38	53	23	91	385	331	476	747
	PME, %				MI, kg kg^{-1}			
ACP	1.54	1.52	-	-	1.20	1.03	-	-
ACP-Cit	1.08	1.12	0.38	-	1.28	1.05	4.84	-
CS-ACP-Cit-8	0.26	0.23	0.23	0.13	2.70	2.59	4.03	1.19
CS-ACP-Cit-12	0.04	0.13	0.17	0.15	5.73	4.43	5.33	1.01
Batch-CS-ACP-Cit	0.26	0.30	0.21	0.13	2.61	1.89	4.27	1.09

The PMI increases when preparing higher composite complexity, as the larger number of process steps needs more ingredients and more water as solvent. This effect is minor for the transition from ACP to ACP-Cit, but is major then to CS-ACP-Cit. The PMIs for the first and the first two steps are on a good industrial process standard, with 28 kg kg^{-1} (ACP) and 34 kg kg^{-1} (ACP-Cit). The latter demonstrates the value of process integration, without separation, in a microreactor flow network. The highest PMI value of 161 kg kg^{-1} is given for CS-ACP-Cit-12, which still is within ranges of reported industrial processes (at three stages); a reduction of the water load here is advised for process optimisation. The E-factor as reverse quotient to PMI mirrors these findings. The MI scores low for all three stages, demonstrating that a good turnover of the resources to the product is made, even for the chitosan addition in the third step. Implicitly, this shows that the main sustainability issue is the reduction of the water use; which is double confirmed by the WI showing a large increase in the third chitosan-adding step.

MI denoted the effect of ingredients dilution, reducing by a factor of 30 the highest PMI values scored in CS-ACP-Cit-8 and CS-ACP-Cit-12 scenarios. PME, as the inverse of PMI, was also very influenced by water usage (WI), especially in highly diluted scenarios.

The specific green chemistry metrics for each ingredient do not follow always the trend of the global metrics, demonstrating that even the ‘product isolation’ with adding more steps, solvent and ingredients (Table 3b) can keep or increase the specific metrics; meaning increasing the functionality per mass unit. The large ‘dilution’ from the second to the third step diminishes the specific metrics of P (and Ca) but the cit-yield improves and the CS-yield is high. The CS-yield is almost quantitative; same for the P-yield for ACP and ACP-Cit and with high Ca-yield for those composites. As citrate is the key ingredient to deliberate P to full performance, the CS addition demonstrates its capability in increasing the performance (cit-content) at good green chemistry values. The large CS related PMI and MI scores demonstrate again the need for a water-resource optimisation in this step.

Continuous-flow made CS-ACP-Cit-8 and batch-made CS-ACP-Cit score almost equal in the specific metrics, Table 3b, as for CS-ACP-Cit-12; with similar trend as the global metrics of these composites.

MI as a water-independent metrics, scores close to optimal (1 kg kg^{-1}) for Ca and P in ACP and ACP-Cit composites, and has favourably low value for CS when used. As for the global values, MI scores throughout all composites better than PMI.

The product mass per time, productivity, was calculated based on Table 3a, Figure 3. It is maximal for the ACP-Cit composite, because the ingredient concentrations could be reduced, when adding Cit and Chi solutions. For the latter, the volume was doubled. Yet, normalizing concentrations obviously would give CS-ACP-Cit-12 scenario the maximum productivity. Under maximum productivity (scenario ACP-Cit), the MI of the process scored 3.89 kg kg^{-1}, while PMI scored 34 kg kg^{-1} pushed by the water use. Then, it can be assumed that scenario CS-ACP-Cit-12 could potentially achieve similar metrics when normalizing concentrations.

Continuous-flow production give higher productivities as batch, Table 3a, by a factor of 1.9 and 2.9 dependent on the composite. The more material is produced, the larger is the difference in composite material produced. The payback is the use of needing more water for the flow process.

3.1.2. Circularity metrics for composites manufacturing

Circularity assessments allow to compute the recycling efficiency needed and to consider the ‘product viewpoint’ beyond assessing the ‘process’ only (see initial remarks in this section), Table 5. To account for product performance (transport to roots without adsorption interference and high P solubility: citric acid content, small size of nano-P), we used the utility factor (U) and lifetime (L), as defined by the Ellen MacArthur Foundation (EMF).[100] Utility reflects product performance increase directly and lifetime indirectly, by allowing to use the same weight-amount of product for a longer time of use. Data about this are unknown, and thus we used a reasonable scenario analysis with increase of U by 10 and 20 % and increase of L by 20 and 40%.

The circularity assessment was performed a gate-to-gate fashion of the process and scaled to 1 ton product. Waste flows were calculated considering the losses *via* formation of by-products or non-recovered reactants, in addition to unrecovered water during separation after centrifugation and subsequent drying. Given the yields described in section 3.1.1, recycling mass flows were calculated considering the liquid fraction after centrifugation, including the corresponding content of unreacted materials and byproducts such as salts.

Assumptions taken were; (i) same performance (utility factor) of the composites; (ii) no side reactions; (iii) unreacted salts are 80 % extracted, as the water recovery was experimentally determined to be 82.5 %; (iv) the liquid fraction with the salts can be reused in the next cycle; and (v) losses include water, sodium salts and 20 % of unreacted materials. Table 4 describes the global mass flows derived from each scenario, which are used to calculate the circular metrics in Table 5.

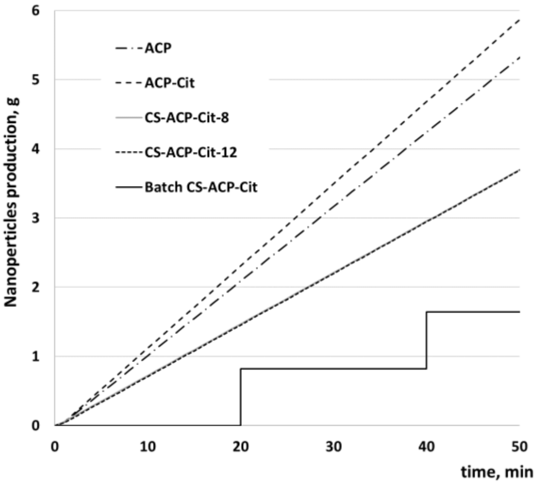

Fig. 3 Productivity of composites manufacturing for continuous-flow and batch processing. Batch synthesis is made in steps, ‘campaigns’, with 20 minutes interval according to the process time needed. In reality, likely discharging, cleaning, charging, will lower substantially batch production.

As for green chemistry metrics, a number of circularity metrics are used to provide a complementary circularity viewpoint. M denotes the mass of all materials needed per production cycle, of which virgin (or new materials, V) are calculated according to the recycling fraction (RF) and the extracted fraction (EF). Waste generated (W) is calculated according to the process losses, and includes an estimation of the fraction to landfill (W0) and the waste generated when recycling (WF). The linear flow index (LFI) and the material circularity indicator (MCI) are calculated using the same data as for the mentioned metrics.

The circularity of the process, denoted by MCI, with recycling is high for all process steps and all composites, scoring in the range of 0.8; with this ratio taken from results of our laboratory experiment. The main conclusion is that recycling, beyond the scope of this paper, is key to achieving circularity. Evidence is that when MCI was computed without recycling, the score dropped to 0.1, as more waste is generated. Another evidence is that when the recycling mass flows, mainly for water, need to be increased, the MCI of the composites CS-ACP-Cit-8 and CS-ACP-Cit-12 turns slightly higher. There is confidence in achieving that goal, because efficient extraction and recycling techniques can be considered, for which high EF and respectively high RF can be assumed. EF was similar in all cases, as the ratio of water recovery and unreacted materials extraction keeps the same. All composites score in the range of RF 80 %. W and V scores become larger with increasing number of process steps, when increasing by-products and water losses; with the most complex composite CS-ACP-Cit-12 scoring highest.

Table 4. *Material mass flows calculated for each scenario normalized to 1 ton nanoparticles production.*

	Materials, t	Recycled, t	Losses, t
ACP	68	54	13
ACP-Cit	81	65	14
CS-ACP-Cit-8	147	120	25
CS-ACP-Cit-12	312	257	54
Batch-CS-ACP-Cit	144	118	25

Table 5. *Circular metrics of composites manufacturing normalized to 1 ton production volume.*

Metrics	ACP	ACP-Cit	CS-ACP-Cit-8	CS-ACP-Cit-12	Batch-CS-ACP-Cit	Units/ Remark
M	68	81	147	312	144	t
RF	0.80	0.80	0.82	0.82	0.82	
V	14	16	26	55	26	t
EF	0.77	0.78	0.79	0.79	0.79	
W	21	24	42	87	41	t
W0	13	14	25	54	25	t
WF	16	18	32	68	32	t
LFI	0.24	0.23	0.22	0.22	0.22	
MCI	0.78	0.79	0.80	0.81	0.80	L=1.0; U=1.0
MCI	0.82	0.83	0.84	0.84	0.80	L=1.2; U=1.0
MCI	0.85	0.85	0.86	0.86	0.80	L=1.4; U=1.0
MCI	0.80	0.81	0.82	0.82	0.80	L=1.0; U=1.1
MCI	0.82	0.83	0.84	0.84	0.80	L=1.0; U=1.2
MCI	0.83	0.88	0.88	0.88	0.80	L=1.4; U=1.2

To account for the product's (composite) higher performance (particle size, citrate content, solubility, distribution; as demonstrated in this study), we adjusted the Intensity Factor U, which is composed in the EMF definition by the Utility Factor F(X); X being Utility and F being Function. EMF defined U means 'performance' (product-related benefit). We assumed 10 or 20 % greater performance, meaning U = 1.1 or 1.2. The demonstrated greater performance will also lead to a longer lifetime L, as less product has to be used to achieve the same outcome in plant growth. We assumed 20 or 40 % longer lifetime, meaning L = 1.2 and 1.4.

3.2. Enhancement in the P availability in soil and P nutrient efficiency of the prepared composites

The P availability in the soil was measured after 14 days in the soil incubation experiments and the results were illustrated in Fig. 4. The amount of P added was the same for all treatments except the control without P addition. There was no statistically difference in the available P level of the soil applied with control (no fertiliser), commercial apatite or sodium citrate. It was ineffective under the separated application of apatite due to its low solubility or citrate ions due to the rapid degradation in the soil. The combination of citrate ion and apatite can produce a different result. This is the case for the P availability in the soil using ACP-Cit as the P content was increased to 49 $mg_P\ kg_{soil}^{-1}$, which is a significant difference with the control condition (p-value<0.05). This is an improvement comparing to previous studies using only hydroxyapatite as fertiliser. Xiong *et al.* reported the use of hydroxyapatite in ultisol/vertisol increased the available P to *ca.* 30 $mg_P\ kg_{soil}^{-1}$. [101] As the citrate/phosphate ratio of the ACP-Cit composite was only at 0.36, the difference between the P availability with this composite that of commercial P fertiliser (63 $mg_P\ kg_{soil}^{-1}$) was insignificant. When that ratio increased to 1, in the case of CS-ACP-Cit-8, the P availability (at 70 $mg_P\ kg_{soil}^{-1}$) was significantly higher than the ACP-Cit and had a similar level available P in soil with the commercial P fertiliser.

From the P availability in the incubation, P releasing efficiency (PRE) of the corresponding fertiliser can be calculated by excluding the available P content in the soil and comparing with the total amount of P applied into the soil, as shown in Fig. 5. The fertilisers behaved significantly different. The commercial apatite powder without any additive could only supply less than 10% of its maximum phosphate content. As phosphate has a low solubility in water, as low as $10^{-52.8}$ at pH 7.6, it was releasing P at a "very slow" rate.[102] With the presence of citrate ion in the composite, as shown in the case of ACP-Cit, the PRE of calcium phosphate significantly increased up 38%, yet this was still lower than that of the commercial product. It will be possible to boost further this efficiency if the citrate content can be increased but this type of composite has reached its maximum citrate content, as explained previously. With the addition of chitosan into the composite, the amount of P released from the fertiliser increased significantly to over 63% of the P nutrient was released into the soil and still available to for plant uptake after 14 days of incubation. The PRE of the reported formulation after 14 days was not much significant compared to the commercial fertiliser but they behaved differently in the soil. For the commercial fertiliser, it is a highly soluble form of phosphorus, the PRE from day 0 would be above 99% as phosphate ion was released when water was applied to the container. In other words, after 14 days, the commercial fertiliser lost nearly half of its nutrient due to fixation and only 55% of its initial phosphorus was available in the soil. For the reported formulation, at day 0, its PRE would be less than 1% as it is a solid fertiliser with limited solubility. If it was also fixated in the soil, then PRE would be significantly lower than the commercial fertiliser. However, we still obtained a comparative %PRE which indicated the phosphate ion released from the solid fertiliser wasn't fixated by soil's cations due to the presence of citrate ions.

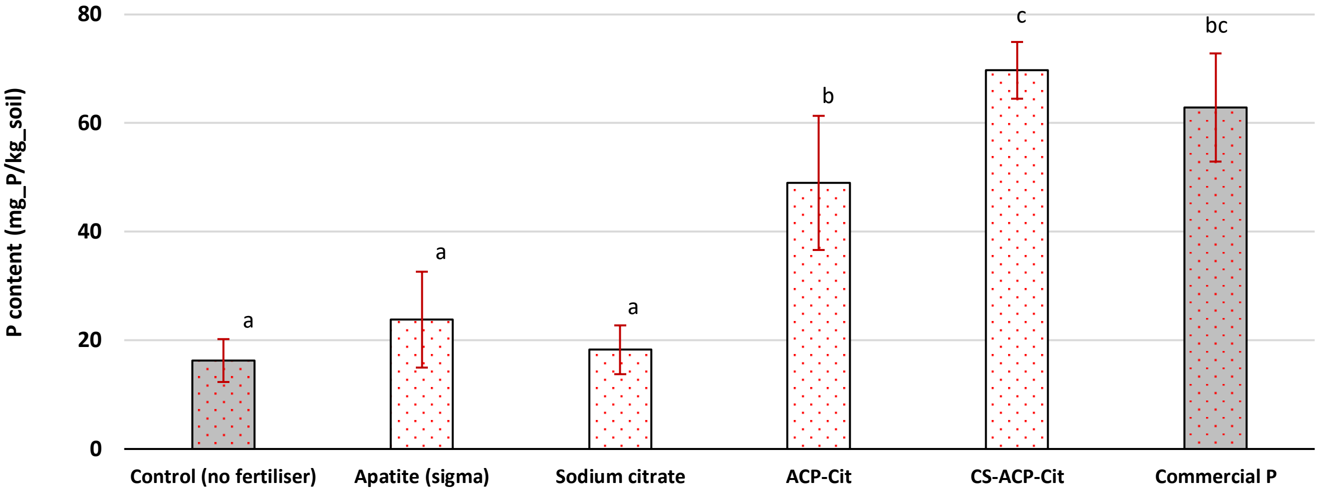

Fig. 4 Phosphorus (P) availability ratio of soil using different fertilizer (application rate: 85 mg_P/kg_{soil}) compared to control (m_P = 0 mg/kg_{soil}). Different letters indicate significant differences among the type of fertilisers used in the soil incubation experiment in the available P content at p-value < 0.05 by one-way ANOVA (Tukey's studentised range test)

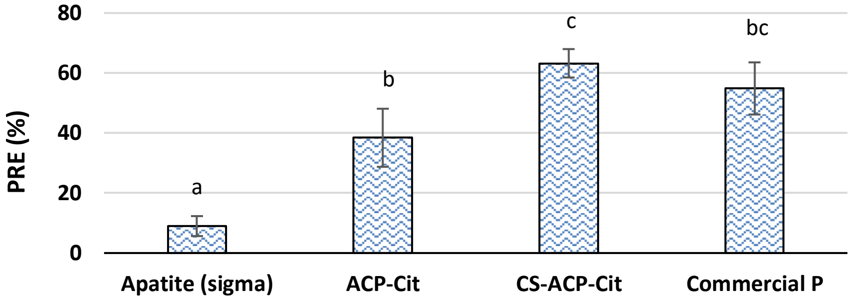

Fig. 5 Phosphorus releasing efficiency (PRE) of different fertilisers. Different letters indicate significant differences among the type of fertilisers used in the soil incubation experiment in the available P content at p-value < 0.05 by one-way ANOVA (Tukey's studentised range test)

3.3 Glasshouse experiment

Two types of wheat were grown in the greenhouse with the aim of studying the efficiency of the composite for enhancing plant P uptake in a P deficient soil. Prior to seed sowing, the soil was amended with a nitrogen at 50 kg N ha^{1-}, potassium at 50 kg K ha^{-1} and P from 0 to 30 kg P ha^{-1}. A second dose of nitrogen (50 kg N ha^{-1}) was later applied at the third week of planting. Two types of wheat were harvested after the third node was detectable (Fig. S6). The parameters that we were investigating in this experiment were the length and dried weight of the shoot and the total P element in the biomass. The P uptake of crop was calculated based on the comparison with plant in the pot with no P fertiliser applied.

The wheat showed no significant differences between pots with different doses of P of the same types of wheat seed but the response was different between the two types, as shown in Fig. 6-a,b. Statistical analysis showed that there was a significant different difference (p-value < 0.05) in the shoot height between type I and II but not between the treatment in the same type (p-value > 0.05). The average shoot height at Day 49 for type I and II are 10.2 ± 0.7 and 12.9 ± 0.9 cm, respectively. Two way ANOVA showed that only the total P uptake in shoot had significant difference (p-value < 0.5) while that of the root was insignificant (Fig. 6-c,d). Furthermore, the interaction between the type of wheat and the application dose was insignificant (p-value > 0.05) in these experiments. With the insignificant change in the height but moderate difference in the total P in the biomass, it was expected to see an improvement in the P uptake and the total plant dry weight, especially for type II wheat (Table 6). The presence of citrate ions in the composite improved the release of phosphate ions and therefore increase the P uptake of wheat as a previous study reported that the uptake of wheat at day 137 was 0.125 mg_P kg_{soil}^{-1} using phosphate rock at the application rate of 50 mg_P kg_{soil}^{-1}.[103] It is also worth noting that the highest dried weight of shoot and root corresponded to the application dose of 32 mg_P kg_{soil}^{-1} which was the lowest application dose of P in the experiment.

3.4. The risk of P leaching

The release of P from ACP-Cit, CS-ACP-Cit and commercial fertiliser was monitored in a vertical soil column experiment containing soil medium. Fig. 7 illustrated the P content in leachate per day. The leachate was compared with that of the control column (no fertiliser). From day 1 to day 7, P was moving from the application position to the bottom of the column, hence, the leachate P did not differ among treatments. Starting from day 8, the commercial fertiliser, had the highest concentration of P in leachate. The two-way ANOVA revealed a statistically significant difference in the P content in the leachate by both the fertiliser type (p-value < 0.05) and the date of watering (p-value < 0.05), and the interaction between these terms was significant (p-value < 0.05). As commercial P is a highly soluble compound, there was a jump in the content of P in the leachate on Day 11, 3.6 µg, and there was an increase in the general trend for leaking P from the column, ending at 1.6 µg. Furthermore, the Tukey *post-hoc* test revealed the significant differences in P content in the leachate between days which translated to an unstable movement of P in the column. The presence of citrate in the ACP-Cit and CS-ACP-Cit-8 samples helped enhancing the solubility of calcium phosphate, although the P concentration in the leachate can be seen to vary significantly between days, ranging from 0.3 to 0.9 µg per day. There was also a period when less 0.2 µg of P was detected (Day 13 to 15) which illustrated the uncontrolled release of P from the composite. The chitosan composite shows a great improvement in term of stability, it releases P with a more constant rate at an averaging rate of approximately 0.7 µg per day (Fig. 7). The Tukey post-hoc test of the P content in leachate by day of the CS-ACP-Cit fertiliser revealed the insignificant differences between day 11 and day 23 which translates to a stable release of phosphate ions in the soil.

The leaching risk of each type of fertiliser can be evaluated *via* the accumulated of P in the leachate, as shown in Fig. 8. The commercial product, due to be a highly soluble salt of P, had a high risk of P leaching. Corresponding to the trend in Fig. 8, the cumulative P in leachate increased rapidly after day 10. In contrast with the commercial product, ACP-Cit sample exhibited the lowest leaching risk among the three types of material in the coil column experiment, but this may result in too low an available concentration of P in the soil. The prepared CS-ACP-Cit sample is the most stable in terms of releasing P in the soil column. While the commercial product and the ACP-Cit exhibited either a “jump” or a “flat” period in the duration of the experiment, the CS-ACP-Cit exhibited a continuous discharge of P. The presence of chitosan is expected to reduce the total amount of phosphate in the leachate, yet in Fig. 8 it was higher than that of ACP-Cit. The increase in the citrate/phosphate ratio can explain this phenomenon as it can help the phosphate ion in the composite to be released more easily *via* ion exchange. Furthermore, the chitosan can play two major functions, to prevent the burst release of phosphate and to protect citrate ions from degradation from soil microbes thus allowing them to gradually exchange with phosphate ions.

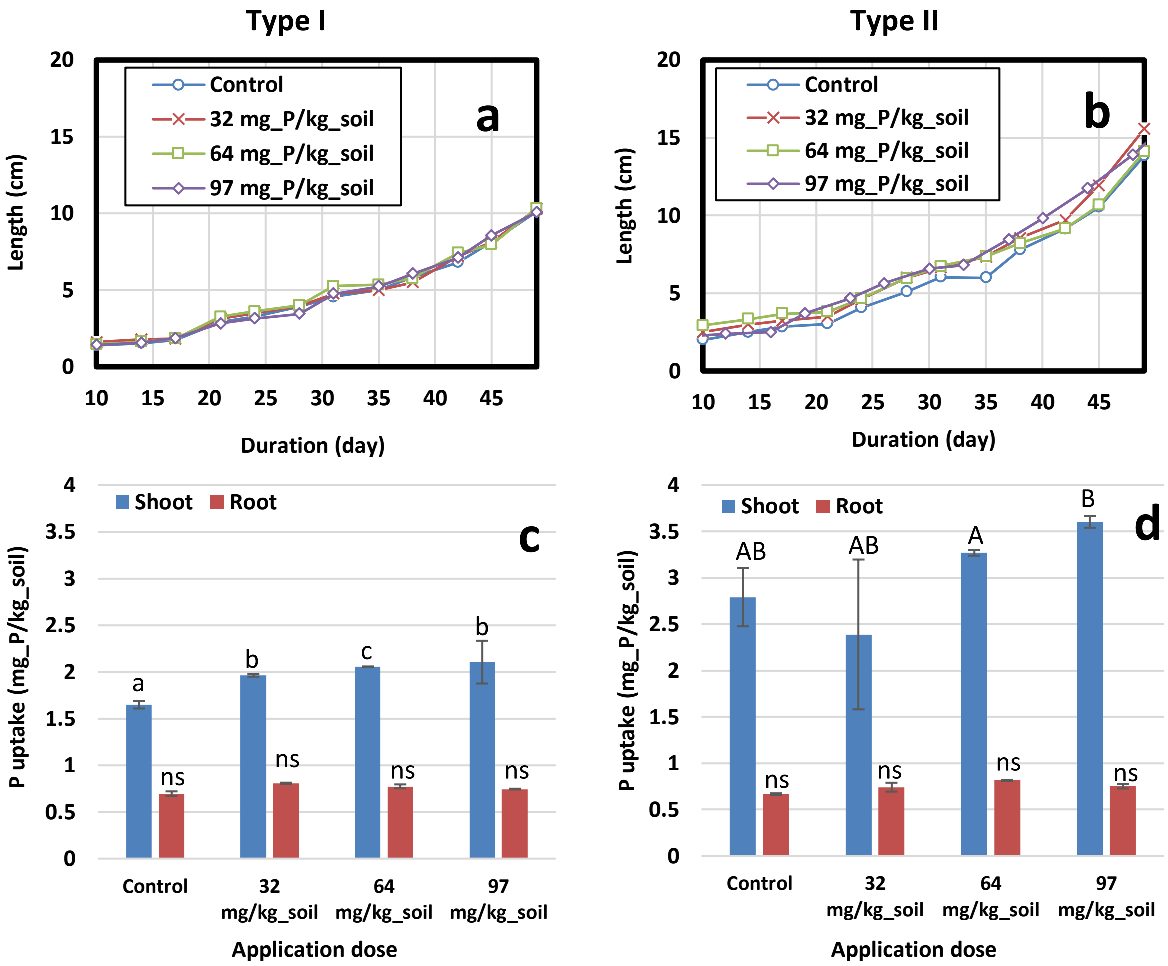

Fig. 6 (Top) Record of wheat height and (bottom) total P uptake in shoot and root for wheats provided by (a,c) laboratory (Type I) and (b, d) farmer (Type II) after day 49. Different letters indicate significant differences among the dose of ACP-Cit used in the experiments at p-value < 0.05 by two-way ANOVA (Tukey’s studentised range test). ns: not significant

Table 6. *Summary of parameters for wheat growing experiments*

Wheat type	P application dose		Shoot P uptake ($mg_P\ kg_{soil}^{-1}$)	Average shoot length (cm)	Total dried shoot weight (g)	Total root dried weight (g)
	$kg_P\ ha^{-1}$	$mg_P\ kg_{soil}^{-1}$				
I	0	0	1.65 ± 0.04^{a}	10.1 ± 1.3^{a}	0.26 ± 0.01^{a}	0.16 ± 0.01^{ns}
	10	32	1.96 ± 0.01^{b}	10.3 ± 2.1^{a}	0.29 ± 0.01^{a}	0.13 ± 0.03^{ns}
	20	64	2.06 ± 0.01^{c}	10.3 ± 1.1^{a}	0.28 ± 0.003^{a}	0.18 ± 0.001^{ns}
	30	97	2.10 ± 0.23^{b}	10.1 ± 1.3^{a}	0.30 ± 0.01^{a}	0.15 ± 0.04^{ns}
II	0	0	2.79 ± 0.31^{AB}	13.8 ± 1.0^{B}	0.46 ± 0.01^{B}	0.12 ± 0.01^{ns}
	10	32	2.39 ± 0.81^{AB}	15.6 ± 1.0^{B}	0.58 ± 0.01^{B}	0.18 ± 0.01^{ns}
	20	64	3.27 ± 0.03^{A}	14.1 ± 2.3^{B}	0.54 ± 0.01^{B}	0.17 ± 0.01^{ns}
	30	97	3.60 ± 0.06^{B}	13.9 ± 1.5^{B}	0.63 ± 0.01^{B}	0.16 ± 0.01^{ns}

Note: ns, not significant. Different letters indicate significant differences among the different treatments at $p < 0.05$ by two-way ANOVA (Tukey's studentised range test)

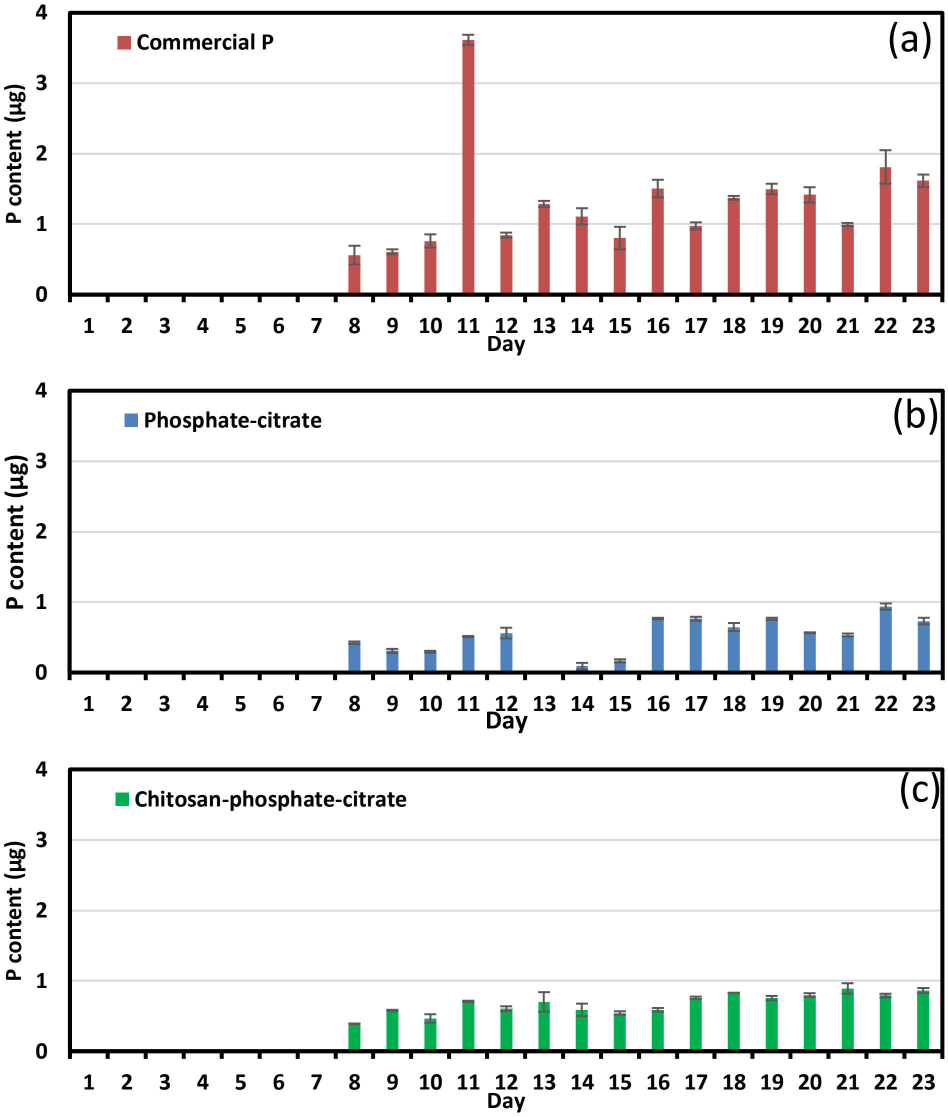

Fig. 7 P content leached by day of different fertilisers: (a) commercial P; (b) phosphate-citrate and (c) chitosan-phosphate-citrate.

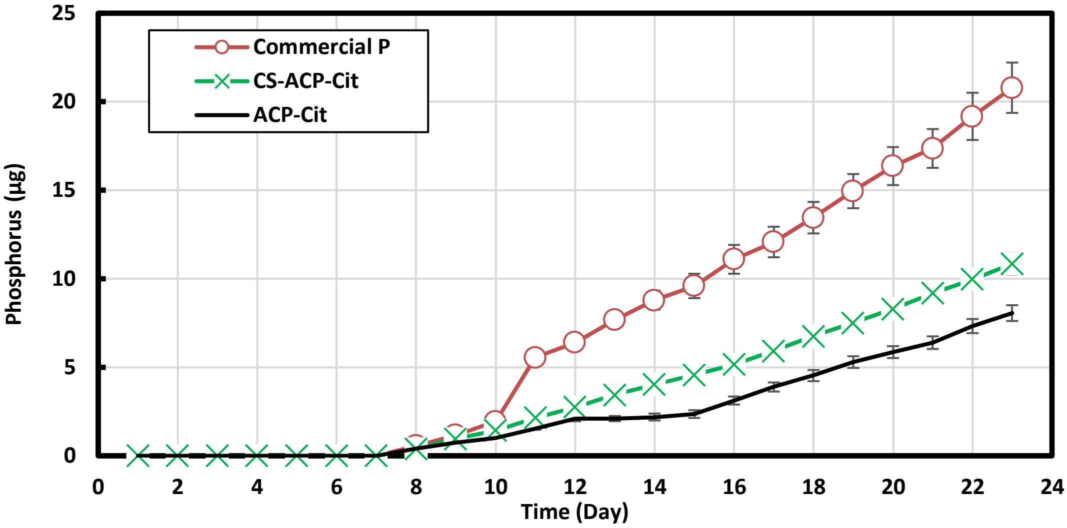

Fig. 8 Accumulated P in leachate of different treatments: commercial P (circle); chitosan-phosphate-citrate (cross) and phosphate-citrate (line)

Conclusion

Taking the idea of applying a limited solubility nanosized P fertiliser and the plants strategy to release low molecular organic acid anions to counter P fixation in soil, this research is one of the first to combine existing single steps into a multireactor network to produce a flow-made fertiliser composite.

In green chemistry metrics, the use of water as solvent largely increases the score of the green chemistry metrics PMI, PME and WI; meaning moderate greenness. The higher water intensity for flow as compared to batch is also due to the reaction network with multiple streams and need to operate the flow system at manageable viscosity to reduce the risk of fouling and high pressure drop. Continuous-flow made CS-ACP-Cit-8 and batch-made CS-ACP-Cit score almost equal in the specific metrics, as for CS-ACP-Cit-12; with similar trend as the global metrics of these composites. Continuous-flow production give higher productivities as batch, by a factor of 1.9 and 2.9 dependent on the composite. The circular assessment shows a recycling factor (RF) of 80% and the material circularity indicator (MCI) scores 0.8, if recycling is considered. Learning is that the circularity has to be improved by the use of higher concentrations of reactants, reducing the use of water. The circularity assessment took account for performance of composites, which is expressed as Intensity Factor (U) and Lifetime (L) in the equation of the Materials Circularity Indicator (MCI). The composites made in this study are performance chemicals, best characterised by circularity metrics, and not classical chemical ‘intermediates’, best characterised by green chemistry metrics.

The prepared formulation is a new material comprising structural and functional complexity and it creates a “performance” as we demonstrated by soil experiments. P release from the prepared composite was as expected: slow release of P and citrate ions in a slow and stable manner. A significant ($p\text{-value} < 0.05$) higher content of available P was observed in the soil incubation experiment with phosphate-citrate and chitosan-phosphate-citrate than in that treated with commercial apatite. In a non-leaching condition, the prepared chitosan-phosphate-citrate composite and the commercial P fertiliser had a similar P releasing efficiency. After 14 days of the incubation experiment, the available P in soil was increased by a factor of 3 compared to soil applied with commercial P and the P releasing efficiency in soil of the prepared fertiliser was 63%. The P uptake of wheat using the ACP-Cit fertiliser was 3.60 ± 0.06 $\text{mg}_\text{P}\ \text{kg}_\text{soil}^{-1}$ and it was higher than previous study using rock phosphate (0.125 $\text{mg}_\text{P}\ \text{kg}_\text{soil}^{-1}$). Shoot length and dried biomass weight were constant within small statistical variation. The soil column experiments revealed that the prepared fertiliser had a significant lower leaching risk and a more stable P releasing behaviour than the commercial P fertiliser. The addition of chitosan increased the citrate content in the fertiliser and thus enhanced the solubility of the solid P particles and further increasing the releasing of P from the fertiliser. This complex product is the proof of concept at scale and it will open door to a commercial application.

Outlook

Future work can focus on the formation of ACP *via* changing the P : citrate ratio to gain control over the morphology and the solubility of the composite. Additional macronutrients (N, K) and micronutrients (Zn, Mn, Cu, etc.) can be introduced into the matrix to further enhance the value of the fertiliser. Further field trials are necessary to investigate the new formular in a realistic scenario and its economic value.

Conflicts of interest

There are no conflicts to declare.

Acknowledgements

The authors acknowledge support from the University of Adelaide, Australia and the University of Nottingham, UK joint PhD program Scholarship, and the Chemical Engineering

Research Fund, the University of Adelaide, Australia for funding this research.

References

1. A. A. Khan, G. Jilani, M. S. Akhtar, S. M. S. Naqvi and M. Rasheed, *J agric biol sci*, 2009, **1**, 48-58.
2. S. Samreen and S. Kausar, *Phosphorus-recovery and Recycling*, 2019, 1-14.
3. S. Chien, L. Prochnow, S. Tu and C. Snyder, *Nutrient Cycling in Agroecosystems*, 2011, **89**, 229-255.
4. T. L. Roberts and A. E. Johnston, *Resources, conservation and recycling*, 2015, **105**, 275-281.
5. T. Daniel, A. Sharpley and J. Lemunyon, *Journal of environmental quality*, 1998, **27**, 251-257.
6. L. Ngatia, J. M. Grace III, D. Moriasi and R. Taylor, *Monitoring of marine pollution*, 2019, 1-17.
7. V. Hessel, M. Escribà-Gelonch, M. K. Sojitra, R. Pranggono, D. Kinasz, C. Zhuang, K. Davey, M. McLaughlin and N. N. Tran, *Green Chem.*, 2023, **25**, 755-770.
8. V. Hessel, M. Escribà-Gelonch, M. K. Sojitra, R. Pranggono, D. Kinasz, C. Zhuang, K. Davey, M. McLaughlin and N. N. Tran, *Green Chemistry*, 2023.
9. S. Sahu and B. Jana, *Ecological Engineering*, 2000, **15**, 27-39.
10. J. Caro and W. Hill, *Journal of agricultural and food chemistry*, 1956, **4**, 684-687.
11. A. Giroto, S. Fidélis and C. Ribeiro, *RSC advances*, 2015, **5**, 104179-104186.
12. N. Kottegoda, C. Sandaruwan, G. Priyadarshana, A. Siriwardhana, U. A. Rathnayake, D. M. Berugoda Arachchige, A. R. Kumarasinghe, D. Dahanayake, V. Karunaratne and G. A. Amaratunga, *ACS nano*, 2017, **11**, 1214-1221.
13. A. H. Kim, C. Y. Anthony, S. H. El Abbadi, K. Lu, D. Chan, E. A. Appel and C. S. Criddle, *Green Chemistry*, 2021, **23**, 4510-4523.
14. D. Kim, T. Wu, M. Cohen, I. Jeon and Y.-S. Jun, *Green Chemistry*, 2018, **20**, 534-543.
15. M. Larsen and S. Jensen, *Archives of oral biology*, 1989, **34**, 957-961.
16. J. S. Duhan, R. Kumar, N. Kumar, P. Kaur, K. Nehra and S. Duhan, *Biotechnology Reports*, 2017, **15**, 11-23.
17. S. R. Mousavi and M. Rezaei, *J Appl Environ Biol Sci*, 2011, **1**, 414-419.
18. S. Manjunatha, D. Biradar and Y. R. Aladakatti, *J farm Sci*, 2016, **29**, 1-13.
19. R. Liu and R. Lal, *Sci. Rep.*, 2014, **4**, 1-6.
20. S. Tang and X. Fei, *ACS Applied Nano Materials*, 2021, **4**, 1364-1376.
21. A. A. Elsayed, E.-G. Ahmed, Z. K. Taha, H. M. Farag, M. S. Hussein and K. AbouAitah, *Scientia Horticulturae*, 2022, **295**, 110851.
22. Y. Chen, P. Rekha, A. Arun, F. Shen, W.-A. Lai and C. C. Young, *Appl Soil Ecol*, 2006, **34**, 33-41.
23. D. L. Jones and P. R. Darrah, *Plant Soil*, 1994, **166**, 247-257.
24. D. Jones, P. Dennis, A. Owen and P. Van Hees, *Plant Soil*, 2003, **248**, 31-41.
25. P. Ryan, E. Delhaize and D. Jones, *Annu. Rev. Plant Biol.*, 2001, **52**, 527-560.
26. T. Darch, M. S. Blackwell, D. Chadwick, P. M. Haygarth, J. M. Hawkins and B. L. Turner, *Geoderma*, 2016, **284**, 93-102.
27. C. S. Paul, F. Mercl, J. Száková, V. Tejnecký and P. Tlustoš, *All Life*, 2021, **14**, 599-609.
28. Y. Wang and H. Lambers, *Plant Soil*, 2020, **447**, 135-156.
29. M. M. Arcand and K. D. Schneider, *Anais da Academia Brasileira de Ciências*, 2006, **78**, 791-807.
30. R. Adeleke, C. Nwangburuka and B. Oboirien, *S. Afr. J. Bot.*, 2017, **108**, 393-406.
31. D. Chouhan and P. Mandal, *International journal of biological macromolecules*, 2021, **166**, 1554-1569.
32. L. M. Angelo, D. França and R. Faez, *Carbohydrate Polymers*, 2021, **257**, 117635.
33. M. M. Iftime, G. L. Ailiesei, E. Ungureanu and L. Marin, *Carbohydrate polymers*, 2019, **223**, 115040.
34. M. Azmana, S. Mahmood, A. R. Hilles, A. Rahman, M. A. B. Arifin and S. Ahmed, *International journal of biological macromolecules*, 2021, **185**, 832-848.
35. M. Rinaudo, G. Pavlov and J. Desbrieres, *Polymer*, 1999, **40**, 7029-7032.
36. I. O. Adisa, V. L. R. Pullagurala, J. R. Peralta-Videa, C. O. Dimkpa, W. H. Elmer, J. L. Gardea-Torresdey and J. C. White, *Environmental Science: Nano*, 2019, **6**, 2002-2030.
37. R. Kumaraswamy, S. Kumari, R. C. Choudhary, A. Pal, R. Raliya, P. Biswas and V. Saharan, *International journal of biological macromolecules*, 2018, **113**, 494-506.
38. R. Kumaraswamy, V. Saharan, S. Kumari, R. C. Choudhary, A. Pal, S. S. Sharma, S. Rakshit, R. Raliya and P. Biswas, *Plant Physiology and Biochemistry*, 2021, **159**, 53-66.
39. C. Pan, J. Qian, C. Zhao, H. Yang, X. Zhao and H. Guo, *Carbohydr. Polym.*, 2020, **241**, 116349.
40. J. Berger, M. Reist, J. M. Mayer, O. Felt, N. Peppas and R. Gurny, *Eur. J. Pharm. Biopharm.*, 2004, **57**, 19-34.
41. M. Pieróg, M. Gierszewska-Drużyńska and J. Ostrowska-Czubenko, *Progress on Chemistry and Application of Chitin and its Derivatives. Polish Chitin Society, Łódź*, 2009, **75**, 3.
42. J. Ostrowska-Czubenko and M. Pieróg, *Progress on Chemistry and Application of Chitin and its Derivatives*, 2010, 33-40.
43. V. Hessel, D. Kralisch, N. Kockmann, T. Noël and Q. Wang, *ChemSusChem*, 2013, **6**, 746-789.
44. S. Marre and K. F. Jensen, *Chemical Society Reviews*, 2010, **39**, 1183-1202.
45. N. Hao, Y. Nie and J. X. Zhang, *Biomaterials science*, 2019, **7**, 2218-2240.
46. T. N. Q. Le, N. N. Tran, M. Escribà-Gelonch, C. A. Serra, I. Fisk, D. J. McClements and V. Hessel, *Chemical Society Reviews*, 2021.
47. W. Ehrfeld, V. Hessel, H. Möbius, T. Richter and K. Russow, *DECHEMA MONOGRAPHIEN*, 1995, 1-28.
48. S. K. Kurt, I. Vural Gürsel, V. Hessel, K. D. P. Nigam and N. Kockmann, *Chem. Eng. J.*, 2016, **284**, 764-777.
49. F. Liu, D. Wang, C. Sun, D. J. McClements and Y. Gao, *Food Chem.*, 2016, **205**, 129-139.
50. L. Zhang, V. Hessel, J. Peng, Q. Wang and L. Zhang, *Chem. Eng. J.*, 2017, **307**, 1-8.
51. M. R. Asrami, N. N. Tran, K. D. P. Nigam and V. Hessel, *Sep. Purif. Technol.*, 2021, **262**, 118289.
52. N. J. Straathof, B. J. Tegelbeckers, V. Hessel, X. Wang and T. Noël, *Chemical Science*, 2014, **5**, 4768-4773.
53. N. J. Straathof, S. E. Cramer, V. Hessel and T. Noël, *Angew. Chem.*, 2016, **128**, 15778-15782.

54. Y. Su, K. P. Kuijpers, N. König, M. Shang, V. Hessel and T. Noël, *Chemistry–A European Journal*, 2016, **22**, 12295-12300.
55. A. Pophali, R. Kajala, H. Ali, N. Verma and K. Nigam, *Reaction Chemistry & Engineering*, 2022, **7**, 719-729.
56. K.-J. Wu, Y. Gao and L. Torrente-Murciano, *Faraday Discuss.*, 2018, **208**, 427-441.
57. K.-S. Chou, Y.-C. Chang and L.-H. Chiu, *Ind. Eng. Chem. Res.*, 2012, **51**, 4905-4910.
58. H. Nakamura, Y. Yamaguchi, M. Miyazaki, H. Maeda, M. Uehara and P. Mulvaney, *Chemical Communications*, 2002, 2844-2845.
59. L. Zhang, W. Xie, S. Guo, X. Xia and S. Yang, *Chemical Engineering and Processing-Process Intensification*, 2023, **184**, 109298.
60. P. Rojahn, V. Hessel, K. D. Nigam and F. Schael, *Chemical Engineering Science*, 2018, **182**, 77-92.
61. Y. He, K.-J. Kim and C.-h. Chang, *Nanomaterials*, 2020, **10**, 1421.
62. A. P. LaGrow, M. O. Besenhard, A. Hodzic, A. Sergides, L. K. Bogart, A. Gavriilidis and N. T. K. Thanh, *Nanoscale*, 2019, **11**, 6620-6628.
63. M. O. Besenhard, A. P. LaGrow, A. Hodzic, M. Kriechbaum, L. Panariello, G. Bais, K. Loizou, S. Damilos, M. M. Cruz and N. T. K. Thanh, *Chem. Eng. J.*, 2020, **399**, 125740.
64. L. Rogers and K. F. Jensen, *Green Chem.*, 2019, **21**, 3481-3498.
65. V. Hessel, *Chemical Engineering & Technology: Industrial Chemistry ‐ Plant Equipment ‐ Process Engineering ‐ Biotechnology*, 2009, **32**, 1655-1681.
66. S. D. Schaber, D. I. Gerogiorgis, R. Ramachandran, J. M. Evans, P. I. Barton and B. L. Trout, *Ind. Eng. Chem. Res.*, 2011, **50**, 10083-10092.
67. S. Lawton, G. Steele, P. Shering, L. Zhao, I. Laird and X.-W. Ni, *Organic Process Research & Development*, 2009, **13**, 1357-1363.
68. M. Iafisco, G. B. Ramírez-Rodríguez, Y. Sakhno, A. Tampieri, G. Martra, J. Gómez-Morales and J. M. Delgado-López, *CrystEngComm*, 2015, **17**, 507-511.
69. J. Prywer, M. Olszynski and E. Mielniczek-Brzóska, *J. Solid State Chem.*, 2015, **231**, 80-86.
70. D. Misra, *Journal of dental research*, 1996, **75**, 1418-1425.
71. F. Piran, Z. Khoshkhoo, S. Hosseini and M. Azizi, *J. Food Qual.*, 2020, **2020**, 1-9.
72. N. Zhang, H. Zhang, R. Li and Y. Xing, *International journal of biological macromolecules*, 2020, **152**, 1146-1156.
73. L. Pastero, M. Bruno and D. Aquilano, *Crystals*, 2018, **8**, 308.
74. X. Jin, J. Zhuang, Z. Zhang, H. Guo and J. Tan, *Journal of colloid and interface science*, 2015, **443**, 125-130.
75. M. A. Martins, C. Santos, M. M. Almeida and M. E. V. Costa, *Journal of colloid and interface science*, 2008, **318**, 210-216.
76. C. Santos, M. M. Almeida and M. E. Costa, *Crystal Growth & Design*, 2015, **15**, 4417-4426.
77. H. Yang, L. Hao, C. Du and Y. Wang, *Rsc Advances*, 2013, **3**, 23184-23189.
78. I. C. Libio, R. Demori, M. F. Ferrão, M. I. Lionzo and N. P. da Silveira, *Materials Science and Engineering: C*, 2016, **67**, 115-124.
79. J. Tanigawa, N. Miyoshi and K. Sakurai, *J. Appl. Polym. Sci.*, 2008, **110**, 608-615.
80. T. Phaechamud, T. Koizumi and G. C. Ritthidej, *Int. J. Pharm.*, 2000, **198**, 97-111.
81. M. C. Bezerra, G. A. Duarte, S. I. Talabi and A. A. Lucas, *Carbohydr. Polym.*, 2022, **278**, 118984.
82. G. B. Ramírez-Rodríguez, G. Dal Sasso, F. J. Carmona, C. Miguel-Rojas, A. Pérez-de-Luque, N. Masciocchi, A. Guagliardi and J. M. Delgado-López, *ACS Applied Bio Materials*, 2020, **3**, 1344-1353.
83. C. A. Serra, B. Cortese, I. U. Khan, N. Anton, M. H. de Croon, V. Hessel, T. Ono and T. Vandamme, *Macromolecular Reaction Engineering*, 2013, **7**, 414-439.
84. M. Escribà-Gelonch, G. D. Butler, A. Goswami, N. N. Tran and V. Hessel, *Plant Physiology and Biochemistry*, 2023, **196**, 917-924.
85. R. Mu, N. Bu, J. Pang, L. Wang and Y. Zhang, *Foods*, 2022, **11**, 3727.
86. S. Vasantham, S. Nagabooshanam, S. Wadhwa and A. Mathur, *Nanoscience for Sustainable Agriculture*, 2019, 659-681.
87. Y. C. Ching and G. Redzwan, *Sustainability*, 2017, **9**, 1062.
88. S. Wu, B. Thapa, C. Rivera and Y. Yuan, *Journal of Environmental Chemical Engineering*, 2021, **9**, 104761.
89. I. S. Hosu, L. Dimitriu, I. Bala, D. Constantinescu-Aruxandei, O. Dima and F. Oancea, *Chemistry Proceedings*, 2022, **7**, 32.
90. H. Menkveld and E. Broeders, *Water Practice and Technology*, 2017, **12**, 514-519.
91. K. W. Jung, T. U. Jeong, B. H. Choi, H. Jeong Kang and K. H. Ahn, *Environ. Prog. Sustain. Energy*, 2017, **36**, 1365-1373.
92. Y. Zheng, B. Wang, A. E. Wester, J. Chen, F. He, H. Chen and B. Gao, *Chem. Eng. J.*, 2019, **362**, 460-468.
93. A. L. Gao and Y. Wan, *Chemosphere*, 2023, **313**, 137434.
94. E. W. Lempinen, Paul Anastas, the Father of Green Chemistry, Urges New, Cleaner Solutions for Past and Future Challenges, https://www.aaas.org/news/paul-anastas-father-green-chemistry-urges-new-cleaner-solutions-past-and-future-challenges, (accessed October, 2010).
95. J. Colwell, *Australian Journal of Experimental Agriculture*, 1963, **3**, 190-197.
96. Y. Chen, W. Gu, H. Pan, S. Jiang and R. Tang, *CrystEngComm*, 2014, **16**, 1864-1867.
97. M. Jahanshahi, A. W. Pacek, A. W. Nienow and A. Lyddiatt, *Journal of Chemical Technology & Biotechnology: International Research in Process, Environmental & Clean Technology*, 2003, **78**, 1111-1120.
98. K. Do Kim and H. T. Kim, *J. Eur. Ceram. Soc.*, 2003, **23**, 833-838.
99. R. Samavini, C. Sandaruwan, M. De Silva, G. Priyadarshana, N. Kottegoda and V. Karunaratne, *Journal of agricultural and food chemistry*, 2018, **66**, 3330-3337.
100. The Ellen MacArthur Foundation, Towards the Circular Economy, https://ellenmacarthurfoundation.org/towards-the-circular-economy-vol-2-opportunities-for-the-consumer-goods, (accessed 2013).
101. L. Xiong, P. Wang, M. N. Hunter and P. M. Kopittke, *Environmental Science: Nano*, 2018, **5**, 2888-2898.
102. J. Kamieniak, P. J. Kelly, C. E. Banks and A. M. Doyle, *Journal of Inorganic and Organometallic Polymers and Materials*, 2018, **28**, 84-91.
103. L. Prochnow, S. Chien, G. Carmona and J. Henao, *Agronomy Journal*, 2004, **96**, 761-768.